

Simulation and experimental on the quick-freezing of diced mango by dry ice spray

Jinghong Ning^{a*}, Sen Zhu^{b*}, Zhipeng Song^c, Ziliang Ren^d, Luyao Sun^e

Tianjin Key Laboratory of Refrigeration Technology, Tianjin University of Commerce, 409 Beichen District Guangrong Road, 300134, Tianjin, China

Abstract: In order to improve the quality of quick-frozen diced mango, a cylindrical quick-frozen container with dry ice spray is designed, the temperature field and velocity field of diced mango sprayed by dry ice in quick-freezing tank are simulated by COMSOL Multiphysics. The effects of different inlet velocities (0.15, 0.20, 0.25, 0.30, 0.35 and 0.40m/s), on the quick-freezing process of diced mango are studied. The results show that with the increase of the inlet velocity of dry ice, the time for diced mango to meet the requirements of quick freezing is continuously shortened, and the outlet solid fraction fluctuates within a certain range. When the inlet velocity is 0.25m/s, the inlet radius is 15mm and the size of diced mango is 10mm, the quick-freezing effect is the best. By the experimental verification, the average errors of surface temperature and core temperature of diced mango to meet the requirements of quick freezing are 3.9% and 3.8% respectively. The results lay a foundation for the popularization and application of dry ice spray quick frozen diced mango.

1. Introduction

Mango is a world-famous tropical fruit, known as the "king of tropical fruits". Mature mango is rich in nutrition, rich in protein, minerals, vitamins, carotenoids and other nutrients^[1]. However, mangoes contain a lot of water and sugar, which are perishable after picking and have a relatively short storage life^[2]. In order to extend the shelf life of mango and maintain its original quality attributes, quick freezing is the most commonly used method at present. A spray rapid freezing device using liquid N₂ or CO₂ to directly spray and freeze appears^[3]. Cheng^[4,5] compared and analyzed the application of numerical simulation technology in food from different aspects, providing a reference for the application of this technology in food freezing. Tan^[6] used high-pressure CO₂ technology to quickly freeze the agaricus bisporus and found that the pressure relief time would affect the quality of the agaricus bisporus. Li^[7] have done a lot of work in spray cooling and simulation experiments, providing theoretical basis for further research. Many foreign scholars^[8,9] studied the liquid nitrogen spray fluidization quick freezing system and its freezing performance, and concluded that the main disadvantage of liquid nitrogen quick freezing is the high operating cost.

The natural working medium, dry ice, namely solid carbon dioxide, has a boiling point of -78.5°C and has a huge latent heat of sublimation, which can take away a large amount of heat in a very short period of time, thus meeting the requirements of quick freezing of food. In

this paper, diced mango were sprayed with dry ice for quick freezing, and a quick freezing tank for diced mango was designed. The temperature field and velocity field of the process of quick freezing diced mango in the quick freezing tank by dry ice spraying were simulated by COMSOL Multiphysics. The simulation results of dry ice spray quick freezing mango were analyzed and compared, and the experimental verification was carried out to obtain the best structure and thermal parameters. It provides a theoretical basis for further research on dry ice quick-frozen mango.

2. Model of Quick Freezing Tank

2.1. Physical model

The size of quick freezing tank is 260mm×430mm (diameter × high), with 4 material trays inside, each of which has a diameter of 200mm, a thickness of 2mm and a spacing of 80mm. The left side of the quick freezing tank is provided with four dry ice inlets and the right side is provided with one carbon dioxide gas outlet (as shown in Fig 1). The inlet radius of dry ice is set to 10, 12, 15, 18 and 20mm respectively, and the outlet radius is set to 30mm. The size of diced mango is set as the cube with the edge length of 5mm, 10mm and 15mm, and the spacing of each diced mango is 10mm. The parameters and characteristics of materials in the model are shown in Table 1.

Corresponding author: ^{a*}ningjinghong@126.com, ^{b*}18037670853@163.com, ^c1329494697@qq.com, ^d972582436@qq.com, ^esunluyao199903@163.com

Table 1. Parameters of the selected materials for the model

Attributes	Constant pressure heat capacity/ $J \cdot (kg \cdot K)^{-1}$	Density/ $(kg \cdot m^{-3})$	Thermal conductivity/ $W \cdot (m \cdot K)^{-1}$	Dynamic viscosity/ $(Pa \cdot s)$	Specific heat rate
Dry ice	770	1562	5	5×10^{-6}	1.374
Gaseous carbon dioxide	Cp(T)	Rho (Pa, T)	K(T)	eta(T)	1.3
Stainless steel	475	7850	44.5	—	—
Mango	3770	1210	0.56	—	—

* CP (T), Rho (Pa, T), K (T) and eta (T) in the table are all functions of the properties of the selected materials, and there are no specific values.

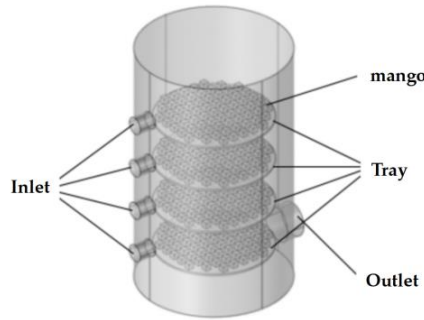


Fig 1. Mode of quick freezing tank



Fig 2. Model grid

COMSOL software is used to mesh the model and calculate the physical field coupling. Considering that the change gradient of the physical quantity is large when the dry ice particles contact the diced mango, it is necessary to carry out intensive grid division around the diced mango. As shown in Fig 2, structural grid is adopted, and the grid quality is above 0.6. Enable the transient solver in COMSOL, set the calculation time to 200 s, the time step to 1 s, and the tolerance factor to 0.5 to solve.

2.2. Calculation method

Assuming that the fluid is incompressible, the physical property of the fluid is constant, there is no internal heat source, and the heat dissipation due to viscous dissipation is negligible, the heat exchange process conforms to the third boundary condition^[10,11]. The diced mango sprayed by dry ice particles and the material tray are forced convection heat exchange.

The heat transfer part of the model is based on the energy conservation equation

$$\rho C_p \frac{\partial T}{\partial t} + \rho C_p u \cdot \nabla T + \nabla q = Q \quad (1)$$

$$q = -k \nabla T \quad (2)$$

Model fluid heat transfer part:

$$\rho C_p \frac{\partial T}{\partial t} + \rho C_p u \cdot \nabla T + \nabla q = Q + Q_p + Q_{vd} \quad (3)$$

$$\rho \nabla \cdot u = 0 \quad (4)$$

By calculation, $Re = 1859 < 2000$, which is laminar flow.

The phase change reference equation is as follows:

$$\rho_p = \theta_1 \rho_1 + \theta_2 \rho_2 \quad (5)$$

$$C_p = \frac{1}{\rho_p} (\theta_1 \rho_1 C_{p,1} + \theta_2 \rho_2 C_{p,2}) + L_{1 \rightarrow 2} \frac{\partial \alpha_m}{\partial T} \quad (6)$$

$$\alpha_m = \frac{1}{2} \frac{\theta_2 \rho_2 - \theta_1 \rho_1}{2 \theta_1 \rho_1 + \theta_2 \rho_2} \quad (7)$$

$$k = \theta_1 k_1 + \theta_2 k_2 \quad (8)$$

The phase change material parameters of the model are shown in Table 2. The formula symbols are explained in Table 4.

Table 2. Parameters of phase change

Parameter name	Value	description
T_p/K	194.65	Phase transition starting temperature
T_{deat}/K	283.15	Phase transition temperature interval
$L_{1 \rightarrow 2}/(J \cdot kg^{-1})$	5.736×10^{-5}	Latent heat of phase transition
T_{us}/K	193.15	Dry ice enters initial temperature
T_0/K	273.15	Model initial temperature

3. Simulation Results

3.1. Influence of inlet velocity of dry ice

The diced mango is pre-cooled to 273.15K before quick freezing, and the inlet velocity of dry ice in the quick freezing tank is set to 0.15, 0.20, 0.25, 0.30, 0.35, and 0.40m/s, respectively. It can be observed that within 20 minutes, the surface and core temperatures of the quick-frozen diced mango reach $-35^\circ C$ and $-18^\circ C$, respectively. The surface and core temperatures required to meet the quick freezing requirements were simulated and calculated using COMSOL software, as shown in Table 3.

Table 3. Comparison of calculation data for different inlet velocity

Inlet velocity/ ($\text{m}\cdot\text{s}^{-1}$)	Time for the surface of diced mango to drop to -35°C/s	Time for the core of diced mango to drop to -18°C/s	Time to pass through the maximum ice crystal formation zone/s	Outlet solid fraction/%
0.15	138	140	50	45
0.20	114	116	37	46
0.25	102	105	35	43
0.30	94	97	31	47
0.35	81	90	26	48
0.40	74	84	20	49

* The entrance radius is 15mm, and the edge length of diced mango is 10mm.

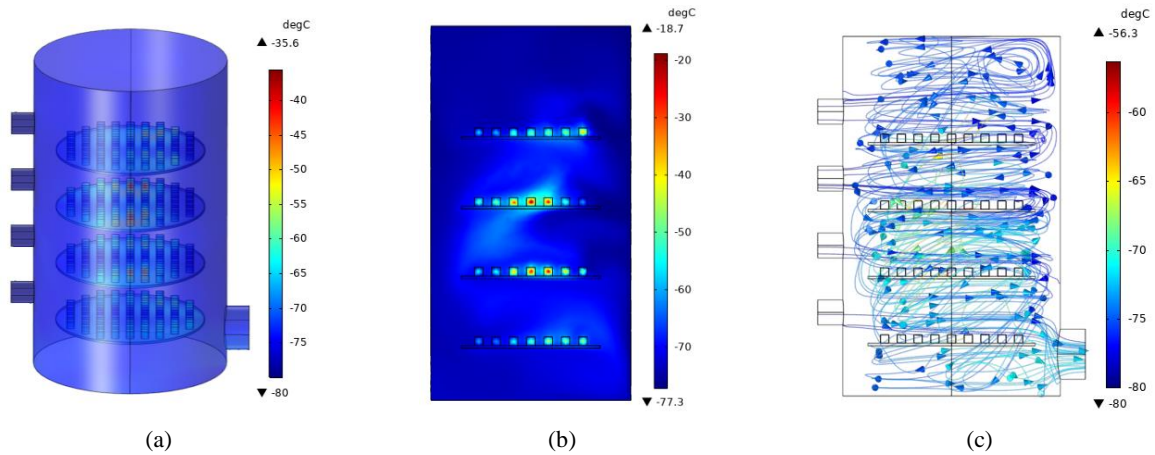
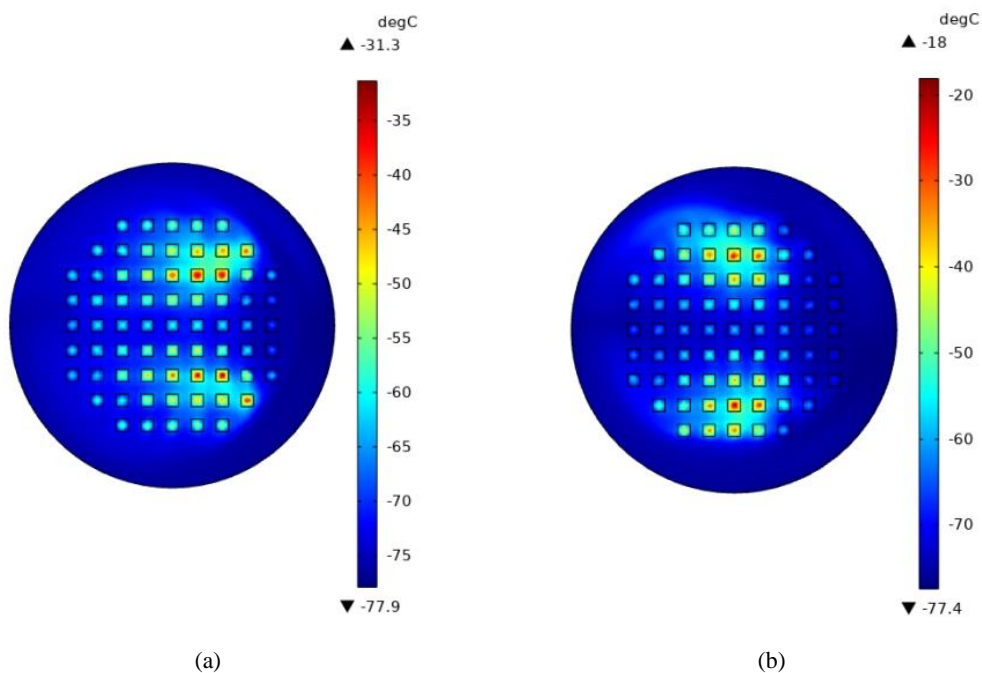


Fig 3. Simulation results of temperature field and velocity field for $t=105\text{s}$. (a) Surface temperature of diced mango; (b) Core temperature of diced mango; (c) Streamline trend and fluid temperature.

3.2. Core temperature of diced mango in each layer

Figure 4 shows the change of core temperature of each layer of diced mango when the inlet radius is 15mm, the

inlet velocity is 0.25m/s , and the edge length of diced mango is 10mm.



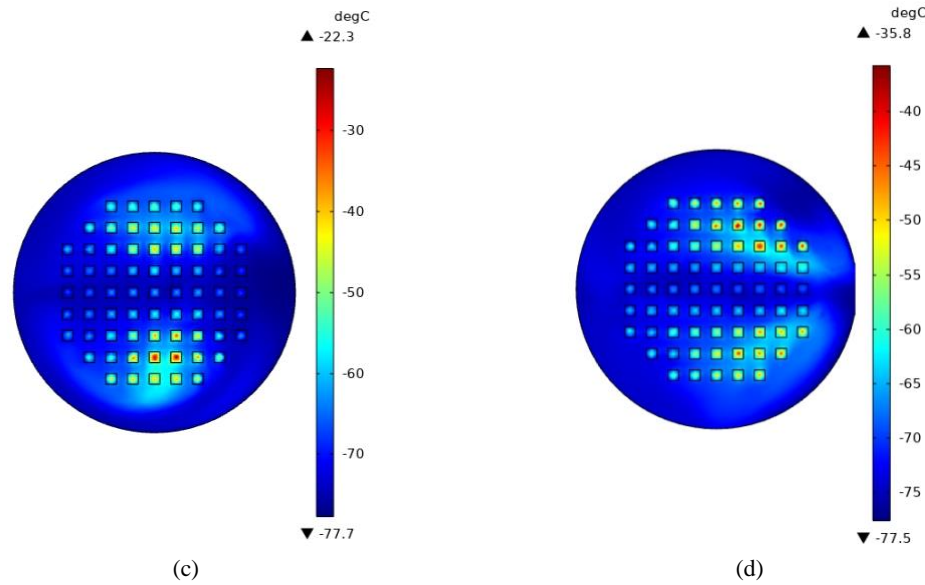


Figure 4. The core temperature of each layer of diced mango when the time is 105s. (a) Core temperature of diced mango on the first layer; (b) Core temperature of diced mango on the second layer; (c) Core temperature of diced mango on the third layer; (d) Core temperature of diced mango on the fourth layer.

4. Discussion and Analysis

The results indicate that under the condition of an inlet radius of 15mm, increasing the inlet velocity leads to a decrease in the core temperature of diced mango to -18°C and the surface temperature to -35°C . In addition, the time required for the diced mango to pass through the maximum ice crystal formation zone decreases. The solid fraction at the outlet fluctuates within a certain range. Excessive freezing rate can cause the diced mango to crack at low temperatures, affecting the quality and appearance of the mango. Lower solid fraction at the outlet corresponds to a lower amount of dry ice inside the quick freezing tank, resulting in a more uniform temperature distribution when the diced mango meets the quick freezing requirements. It also reduces operating costs. Taking into account these factors, it can be concluded that an inlet velocity of 0.25m/s achieves the optimal freezing effect. The simulation results of the temperature field and velocity field are shown in Fig 3, where Fig 3c depicts the variation trend and temperature distribution of the fluid inside the quick freezing tank.

It can be seen from Figure 4 that at the same time, the core temperature of the second layer of diced mango is relatively high, and the core temperature of the fourth layer of diced mango is relatively low, and the quick freezing effect of diced mango in the middle area of each layer is better than that of both sides. The reason is that after the dry ice is injected into the quick freezing tank, there is a core area with uniform velocity in the core of the jet. With the forward movement of the fluid, the core area continues to shrink, and finally the velocity section shows a distribution of large in the middle and gradually decreasing at the edge. After the dry ice reaches the inner wall of the quick freezing tank, it spreads around along the inner wall to form a wall attached jet zone. After the dry ice reaches the wall surface, it will generate disturbance, and the local heat transfer intensity of the

impacted wall surface is high, while the other areas are relatively low. The flow and disturbance of each layer of dry ice are different, resulting in different amount of dry ice contacted by each layer of diced mango, so the temperature change is also different. The quick freezing time is 105s, and the core temperature of all diced mango has dropped below -18°C , which meets the requirements of quick freezing. Therefore, an inlet velocity of 0.25m/s is the better choice for the quick freezing model, considering an inlet radius of 15mm and diced mango with an edge length of 10mm.

5. Experimental Study

5.1 Dry ice spraying system

The schematic diagram of dry ice spraying system is shown in Fig 5, which is mainly composed of carbon dioxide cylinder, pressure reducing valve, flow regulating valve, flowmeter, dry ice nozzle, quick freezing tank and data acquisition system. To increase the percentage of dry ice particles obtained, the carbon dioxide cylinder is inverted. Open the valve of the carbon dioxide cylinder, the liquid carbon dioxide flows out of the cylinder, flows through the pressure reducing valve, the temperature drops sharply and reaches the gas-solid boundary, forming dry ice particles, which can be explained by the Joule Thomson expansion effect, and then flows through the flow regulating valve and flowmeter to the dry ice nozzle, which is connected to the inlet of the quick freezing tank, and the dry ice particles enter the quick freezing tank through the nozzle, sublimation takes away the heat of the mango^[12], causing it to freeze. The carbon dioxide gas generated is discharged from the outlet of the quick freezing tank.

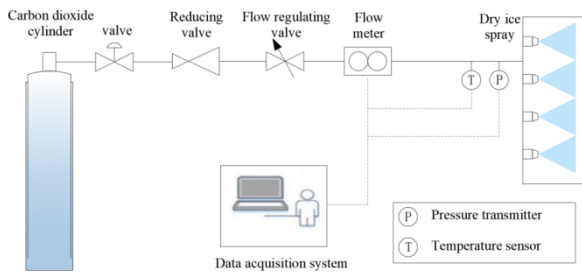


Fig 5. Schematic diagram of dry ice spraying system

5.2 Results and analyzing

As shown in Fig 6, the device diagram of dry ice spraying quick freezing mango dice is shown, Fig 7 is the experimental photo. According to the simulation results, set the entrance radius, entrance velocity and mango size respectively. During the experiment, T-type thermocouples were inserted into the core and surface of diced mango respectively, and the thermocouples were connected to Yokogawa GP10 data collector. The temperature change and freezing temperature curves were displayed, recorded and drawn automatically by the computer. The experiment ended when the diced mango with the slowest temperature drop in the quick freezing tank reached the requirements for quick freezing.



Fig 7. Experimental photo

After several groups of experiments, the experimental data were collated and analyzed, and the experimental results were compared with the simulation results, as shown in Fig 8. At 109s, the core temperature of diced mango all reached -18°C , with an error of 3.8% from the simulation result of 105s. At 106s, the surface temperature of diced mango all reached -35°C , with an error of 3.9% from the simulation results of 102s. The main reasons for the error are: (1) The diced mango in the experiment is cut by hand, and the size is uneven. The closer the size of diced mango to the size set in the simulation, the smaller the error of the experiment results. (2) The operation error exists in the insertion position of the thermocouple at the core and surface of the mango cone, which makes the experimental results have errors. (3) The shelf of material tray interferes with the turbulence of dry ice and affects the effect of quick freezing.

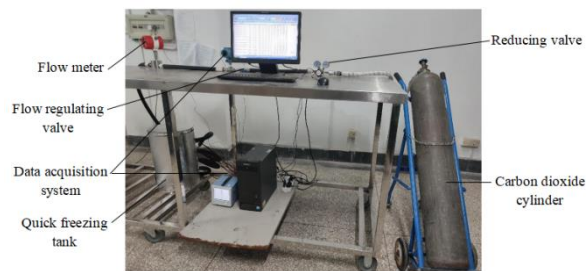


Fig 6. Dry ice spray quick freezing device

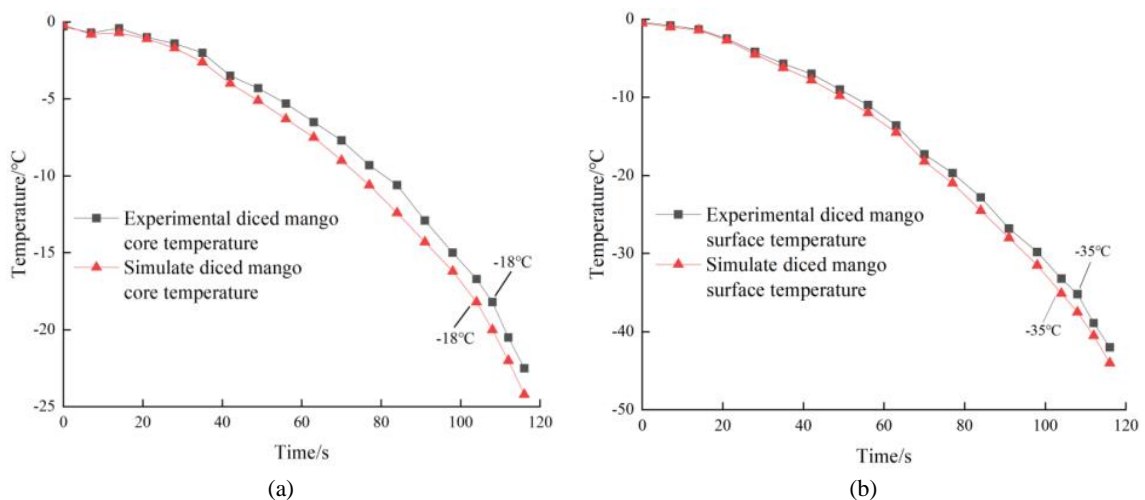


Fig 8. Temperature change of diced mango. (a) Core temperature change; (b) Surface temperature change

6. Conclusion

By the numerical simulation and experiment of dry ice jet quick freezing of diced mango and the comparison with the existing quick freezing methods of diced mango, the following conclusions can be drawn:

(1) By setting different inlet velocity, it can be seen that with the increase of inlet velocity, the time for diced mango to meet the requirements of quick freezing is continuously shortened, and the outlet solid fraction fluctuates within a certain range. When the inlet velocity is 0.25m/s and the inlet radius is 15mm, the time to pass through the maximum ice crystal formation zone is shorter, the solid phase fraction at the outlet is the lowest, the dry ice is less accumulated in the quick freezing tank, the utilization rate is higher, the temperature distribution of diced mango is uniform, and the quick freezing quality is better.

(2) By experimental verification, the average errors of the core temperature and surface temperature of diced mango meeting the requirements of quick freezing are 3.8% and 3.9% from the simulation results respectively. The error is caused by the uneven size of the experimental diced mango, the insertion position error of the thermocouple and the interference of the shelf of the material tray with the dry ice turbulence.

Table4. Naming of formula symbols

Nomenclature	
ρ	Density of material, kg/m ³
C_p	Specific heat capacity of phase change materials, J/(kg·K)
T	Fluid temperature, K
t	Time, s
u	Actual inlet velocity, m/s
q	Convective heat flux, W/m ²
k	Thermal conductivity of phase change materials, W/(m·K)
Q	Enthalpy of dry ice, J/kg
Q_p	Internal energy of dry ice, J/kg
Q_{vd}	Kinetic energy of dry ice, J/kg
v	Flow rate of fluid, m/s
d	Feature length, m
μ	Dynamic viscosity, Pa·s
ρ_1, ρ_2	Density of two materials before and after phase transformation, kg/m ³
θ_1, θ_2	Volume fraction of two phase change materials
k_1, k_2	Thermal conductivity of two phase change materials
α_m	Mass fraction

Acknowledgements

The project was supported by the Tianjin University Student Innovation Training Program "Study on Dry Ice Spray Quick Freezing System for Fruits and Vegetables"(NO.202110069071).

References

1. Quanguang, H.E., Meihua, H., Ezhen, Z., Ming, X., Ming, D., & Zhenyong, H, et al. (2017). Comparative study on different varieties of mango pieces texture properties after liquid nitrogen quick freezing and thawing. *Chinese Journal of Tropical Crops*.
2. Zhang, Y., Zhao, J. H., Ding, Y., Xiao, H. W., Sablani, S. S., Nie, Y., ... & Tang, X. M. (2018). Changes in the vitamin C content of mango with water state and ice crystals under state/phase transitions during frozen storage. *Journal of Food Engineering*, 222, 49-53.
3. Song, J., Zheng, M., Wang, Y., Yao, F., & Yu, Z. (2019). The current situation analysis of quick freezing technique, equipment and quality control for fruits and vegetables in China. *Storage and Process*, 19(3), 154-161.
4. Cheng, F., Yang, X., You, Z., & Hong, H. (2014). Application of numerical simulation in the research of food freezing process. *Nongye Jixie Xuebao= Transactions of the Chinese Society for Agricultural Machinery*, 45(7), 162-170.
5. Khuwijitjaru P, Somkane S, Nakagawa K, et al. (2022). Osmotic dehydration, drying kinetics, and quality attributes of osmotic hot air-dried mango as affected by initial frozen storage[J]. *Foods*, 11(3): 489.
6. Tan, X., Wu, J., Liao, X., Pang, X., & Sun, Z. (2011). Optimization on quick freezing technology of agaricus bisporus by high pressure carbon dioxide. *Transactions of the Chinese Society of Agricultural Engineering*, 27(3), 375-380.
7. Li, J. X., Li, Y. Z., Li, E. H., & Cai, B. Y. (2020). Experimental investigation of spray-sublimation cooling system with CO₂ dry-ice particles. *Applied Thermal Engineering*, 174, 115285.
8. Lemus-Mondaca, R. A., Vega-Gálvez, A., & Moraga, N. O. (2011). Computational simulation and developments applied to food thermal processing. *Food Engineering Reviews*, 3, 121-135.
9. Guo, X. F., & Tao, L. R. (2003). Investigation on Freezing Characteristic of LN~ 2-Spraying Fluidized Cooling System. *Journal of Engineering Thermophysics*, 24(3), 475-477.
10. Zhao, Y., Ning, J., & Sun, Z. (2022). Study on liquid nitrogen and carbon dioxide combined jet quick-frozen strawberry. *International Journal of Refrigeration*, 136, 1-7.
11. Zhao, Y., Ning, J., & Sun, Z. (2022). Establishment and experimental verification of temperature prediction model for quick-frozen strawberry jetted with dry ice. *Journal of Food Process Engineering*, 45(9), e14098.
12. Ozdemirli N, Kamiloglu S. (2023). Changes in bioaccessibility of citrus polyphenols during industrial freezing process[J]. *International Journal of Food Science & Technology*, 33, 80-85+90.